# Updated Bayesian Analysis of 3I/ATLAS (C/2025 N1): Loeb-Scale Anomalies, Joint Probabilities, and the Case for Intentional Origin

Julio C. Spinelli Independent Researcher

November 23, 2025

#### Abstract

We present an updated Bayesian analysis of the thirteen anomalies highlighted by Loeb for the interstellar object 3I/ATLAS (C/2025 N1), using his November 2025 re-ranking and probability assignments ("Anomalies of 3I/ATLAS organized by likelihood"). These anomalies span orbital geometry and timing (a retrograde, nearly ecliptic trajectory; fine-tuned multi-planet targeting; and a forecasted Jupiter encounter near the Hill radius), morphology (persistent sunward and anti-solar jets, tightly collimated and unsmeared by rotation), photometry (unusually rapid brightening and blue color near perihelion), composition (a CO<sub>2</sub>-dominated coma with only  $\sim 4\%$  water by mass and extreme Ni/Fe and Ni/CN ratios), polarization (unprecedented negative polarization), and dynamics (non-gravitational acceleration near perihelion requiring large mass loss while the nucleus remains intact). We map Loeb's quoted single-event probabilities—ranging from  $4 \times 10^{-5}$  for the Jupiter Hill-radius fine-tuning to conservative upper bounds of 10% for the least constrained "minor" anomalies—into a joint probability distribution, propagate uncertainties with Monte Carlo sampling, and fold in survey selection and cross-domain correlation factors. Under independence, the joint probability of all thirteen anomalies is  $P_{\rm joint} \simeq 2.4 \times 10^{-30}$ , corresponding to an inflation factor  $k_{\rm req} \simeq 4.2 \times 10^{29}$  natural trials to make such an object likely once. Even generous natural correlations and optimistic discovery opportunities require combined inflation factors  $K_{\rm nat} \gtrsim 10^{17}$  to approach a  $\gtrsim 1\%$  plausibility level, and our Monte Carlo sensitivity analysis finds zero exceedances of this threshold across  $5 \times 10^4$  realizations for multiple  $N_{\rm eff}$  values in both baseline and stress configurations. Intentional origin therefore remains a parsimonious common-cause hypothesis unless future work uncovers a natural mechanism that coherently spans geometry, timing, morphology, chemistry, polarization, and dynamics. This version of the paper explicitly incorporates Loeb's updated anomaly list and probabilities and supersedes earlier analyses based on the original twelve-anomaly set.

#### Plain-language summary (for non-specialists)

3I/ATLAS is a small object from outside our Solar System that passed through in 2025. At first it looked like a strange comet, but as astronomers collected more data, it showed many unusual features at the same time. Its path through space is almost perfectly lined up with the plane of the planets; it flew close to several planets in a "just so" way and is forecast to skim past Jupiter near the edge of its gravitational sphere of influence; its gas is rich in carbon dioxide and nickel but poor in water and iron; its light is polarized in an extreme way; its jets seem to push both toward and away from the Sun; and its motion suggests strong jets without the object breaking apart.

Each of these oddities might be rare but still natural on its own. In this paper we ask a simple question: how likely is it that all of them happen together just by chance? Using standard probability tools and computer simulations, we combine the odds for each unusual feature and also allow for generous ways in which some of them might be related. Even under assumptions that strongly favor a natural explanation, the chance that a random interstellar object would look as strange as 3I/ATLAS is extremely small. Our updated analysis, using Loeb's November 2025 probabilities for thirteen anomalies, drives this combined probability down to roughly one in  $4 \times 10^{29}$ .

A dice analogy helps. With a normal 6-sided die, the chance that you get the *same* number on all 20 throws is about one in  $3.6 \times 10^{15}$  (roughly one in three million billion). With a 20-sided die, the chance that the same face appears on all 20 throws is about one in  $5 \times 10^{21}$ . The updated combined anomalies of 3I/ATLAS are far less likely than those events under the natural assumptions we test. Our results do not prove that 3I/ATLAS was designed by someone, but they show that either we have witnessed a remarkable fluke of nature or we should seriously consider the possibility of intentional origin.

### 1 Introduction

The discovery of 3I/ATLAS (C/2025 N1) by the ATLAS survey (Seligman et al., 2025; Bolin et al., 2025) marks the third confirmed interstellar object (ISO), following 1I/'Oumuamua and 2I/Borisov. Unlike its predecessors, 3I/ATLAS exhibits an unprecedented cluster of rare or anomalous properties across orbital, photometric, morphological, chemical, polarimetric, and dynamical domains (Hibberd et al., 2025; Jewitt et al., 2025; Santana-Ros et al., 2025; Cordiner et al., 2025; Xing et al., 2025; Rahatgaonkar et al., 2025; Puzia et al., 2025; Hoogendam et al., 2025; Gray et al., 2025; Tonry et al., 2025; Cloete et al., 2025; Keto and Loeb, 2025; Zhang, 2025).

Recent work has organized these peculiarities into a list of anomalies for 3I/ATLAS, each with an associated rarity estimate (Loeb, 2025a,c,b). In November 2025 Loeb published an updated ranking and probability assignment, "Anomalies of 3I/ATLAS organized by likelihood", which expands and refines the anomaly set to thirteen items across three categories (major, medium, and minor anomalies).(Loeb, 2025d) In parallel, the Loeb Scale (Eldadi and Loeb, 2025; Trivedi and Loeb, 2025) has been proposed as a framework for classifying interstellar objects based on the strength and combination of their anomalies, with 3I/ATLAS assigned a level comparable to, or higher than, that of 1I/'Oumuamua.

Dynamical reconstructions suggest that 3I/ATLAS may be billions of years older than the Solar System and originate from a distant, low-metallicity environment (Taylor et al., 2025; De la Fuente Marcos and De la Fuente Marcos, 2025). Whether its anomalies can be reconciled with natural cometary physics, or instead require intentional origin, is therefore of broad interest both for planetary science and for the emerging field of technosignature studies.

In this paper we treat the thirteen updated Loeb anomalies as events  $E_1, \ldots, E_{13}$ , assign independent probabilities  $P_i$  anchored in Loeb's quoted estimates and the underlying observational literature, and then combine them within a Bayesian framework. We explore how joint probabilities change under different assumptions about cross-domain correlations and survey selection, and we compare the resulting selection-adjusted probabilities against thresholds motivated by the Loeb Scale.

# 2 Materials and Methods

#### 2.1 Definition of Anomalies

We adopt thirteen anomalies  $(E_1-E_{13})$  closely following Loeb's updated list, split into major, medium, and minor categories, with references to the underlying observational papers where possible:

#### I. Major anomalies with no simple explanation

1. Hill-radius perijove fine-tuning. The forecasted perijove distance of 3I/ATLAS during its encounter with Jupiter on 2026 March 16 is 53.445 ± 0.06 million kilometers,

<sup>&</sup>lt;sup>1</sup>https://medium.com/@avi-loeb/anomalies-of-3i-atlas-organized-by-likelihood-af20fb3b6d21

essentially identical to Jupiter's Hill radius of 53.502 million kilometers. This match was enabled by the non-gravitational acceleration that 3I/ATLAS displayed near perihelion. Loeb assigns a probability  $P_1 = 4 \times 10^{-5}$  for such a coincidence under natural dynamics.

- 2. Fine-tuned arrival time and multi-planet targeting. The arrival epoch was such that 3I/ATLAS passed within tens of millions of kilometers of Mars, Venus, and Jupiter and was near-perihelion when it remained unobservable from Earth because of solar glare (Hibberd et al., 2025; Zhang, 2025). Loeb quotes a likelihood  $P_2 = 5 \times 10^{-5}$  for such timing and geometry under natural assumptions.
- 3. Massive nucleus and high speed. The inferred nucleus is roughly a million times more massive than that of 1I/'Oumuamua and a thousand times more massive than that of 2I/Borisov, while 3I/ATLAS also moves faster than both (Seligman et al., 2025; Bolin et al., 2025; Jewitt et al., 2025; Cloete et al., 2025). Loeb states that the likelihood for such an outlier in mass and speed is  $P_3 < 10^{-3}$  given current ISO statistics; we conservatively adopt  $P_3 = 10^{-3}$ .
- 4. Persistent sunward jet / forward beam. During July and August 2025, and again through November, 3I/ATLAS displayed a prominent sunward jet (anti-tail) that cannot be explained as a purely geometric projection effect as in familiar comets (Jewitt et al., 2025; Santana-Ros et al., 2025; Keto and Loeb, 2025). HiRISE imaging near the Mars encounter confirmed a glowing extension ahead of the object along its direction of motion. Loeb regards such a configuration as having likelihood  $P_4 < 10^{-3}$ ; we adopt  $P_4 = 10^{-3}$ .
- 5. Ni-rich plume and anomalous Ni/CN. Spectroscopy reveals strong nickel emission with little or no corresponding iron, and a Ni/CN ratio orders of magnitude above that of all known comets, including 2I/Borisov (Rahatgaonkar et al., 2025; Puzia et al., 2025; Hoogendam et al., 2025). Loeb notes that this composition resembles industrial nickel alloys and assigns  $P_5 < 10^{-3}$ ; we adopt  $P_5 = 10^{-3}$ .
- 6. Retrograde trajectory aligned with the ecliptic. 3I/ATLAS follows a highly hyperbolic orbit ( $e \sim 6.1$ ) with inclination  $i \simeq 175^{\circ}$ , so that its retrograde trajectory is aligned to within  $\sim 5^{\circ}$  of the planetary ecliptic (Seligman et al., 2025; Hibberd et al., 2025). Loeb assigns a likelihood  $P_6 = 2 \times 10^{-3}$  for such alignment under an isotropic arrival model.

#### II. Medium anomalies, which could be statistical flukes

- 7. Arrival from near the "Wow!" signal direction. The inbound direction of 3I/ATLAS lies within  $\sim 9^{\circ}$  of the sky location of the historic "Wow!" radio signal. Loeb estimates a chance-coincidence probability  $P_7 = 6 \times 10^{-3}$  for such alignment on the sky (Loeb, 2025b).
- 8. Extreme negative polarization. Polarimetric observations show unusually strong negative polarization at phase angles where Solar System comets exhibit much smaller

values (Gray et al., 2025). Loeb quotes a likelihood  $P_8 < 10^{-2}$  when compared to the existing comet polarization database; we adopt  $P_8 = 10^{-2}$ .

#### III. Minor anomalies, potentially explainable by a unique origin

- 9. Only  $\sim 4\%$  water by mass. JWST and related analyses show that the gas plume is  $\rm CO_2$ -dominated with a  $\rm CO_2/H_2O$  mixing ratio  $\sim 8:1$  and an inferred water mass fraction of only a few percent (Cordiner et al., 2025; Xing et al., 2025). Loeb regards this as a minor anomaly and specifies  $P_9 < 0.1$ ; we adopt  $P_9 = 0.1$ .
- 10. Fast brightening and blue color near perihelion. Near perihelion, 3I/ATLAS brightened faster than any previously catalogued comet and exhibited a spectrum bluer than the Sun (Tonry et al., 2025; Zhang, 2025). Loeb labels this a minor anomaly with  $P_{10} < 0.1$ ; we adopt  $P_{10} = 0.1$ .
- 11. Jet energetics requiring large surface area. The observed sunward and anti-solar jets would require an unreasonably large active surface area to absorb enough sunlight to sublimate the required mass flux if powered solely by solar heating (Keto and Loeb, 2025; Cordiner et al., 2025). Loeb assigns  $P_{11} < 0.1$ ; we adopt  $P_{11} = 0.1$ .
- 12. **Tightly collimated jets unsmeared by rotation.** Multiple jets maintain tight collimation and fixed orientation over projected distances exceeding a million kilometers, in spite of measured rotational motion (Santana-Ros et al., 2025; Gray et al., 2025; Loeb, 2025a). Loeb quotes  $P_{12} < 0.1$ ; we adopt  $P_{12} = 0.1$ .
- 13. Non-gravitational acceleration with intact nucleus. Near perihelion, 3I/ATLAS exhibits a non-gravitational acceleration that, if attributed to outgassing, implies the loss of at least  $\sim 13\%$  of its mass over a short interval (Cloete et al., 2025; Loeb, 2025c). HST and other imaging, however, show no breakup or fragmentation of the nucleus (Jewitt et al., 2025). Loeb treats this as a minor anomaly with  $P_{13} < 0.1$ ; we adopt  $P_{13} = 0.1$ .

# 2.2 Probability Assignments

Independent probabilities  $(P_i)$  for each anomaly are initialized from Loeb's updated estimates, then embedded in a parametric uncertainty model. Specifically, we set

$$P_1 = 4 \times 10^{-5},$$
  $P_2 = 5 \times 10^{-5},$   $P_3 = 10^{-3},$   $P_4 = 10^{-3},$   $P_5 = 10^{-3},$   $P_6 = 2 \times 10^{-3},$   $P_7 = 6 \times 10^{-3},$   $P_8 = 10^{-2},$   $P_9 = 10^{-1},$   $P_{10} = 10^{-1},$   $P_{11} = 10^{-1},$   $P_{12} = 10^{-1},$   $P_{13} = 10^{-1}.$ 

These values are not meant as exact frequencies but as nominal means for our uncertainty distributions. For each anomaly  $E_i$  we draw  $P_i$  from a Beta distribution with mean equal to the nominal value and coefficient of variation of 50%, truncated to remain within physically

reasonable bounds. This procedure reflects both the limited sample of ISOs and the statistical uncertainty in mapping Loeb's qualitative statements (e.g. "P < 0.001" or "P < 0.1") to quantitative priors.

The observational literature is used to verify plausibility and define event boundaries (Seligman et al., 2025; Bolin et al., 2025; Jewitt et al., 2025; Cordiner et al., 2025; Rahatgaonkar et al., 2025; Puzia et al., 2025; Xing et al., 2025; Santana-Ros et al., 2025; Gray et al., 2025; Manzano-King et al., 2025; Hoogendam et al., 2025; Hibberd et al., 2025; Taylor et al., 2025; De la Fuente Marcos and De la Fuente Marcos, 2025; Keto and Loeb, 2025; Zhang, 2025; Cloete et al., 2025; Eldadi and Loeb, 2025; Trivedi and Loeb, 2025; Loeb, 2025a,c,b).

### 2.3 Model Building: Takes 1–4

We analyze four model classes, using the thirteen anomalies defined above as the event set:

- Take 1: Full independence of all thirteen anomalies.
- Take 2: Grouped correlations (geometry/targeting, morphology/polarization/photometry, chemistry/composition/dynamics).
- Take 3: Addition of survey selection ( $N_{\text{eff}}$  from ATLAS, ZTF, Pan-STARRS, MPC).
- Take 4: Hypothetical cross-domain couplings beyond known physics.

For Take 2 we use multiplicative correlation factors for three broad domains:

$$C_{\text{geo}}, \quad C_{\text{morph}}, \quad C_{\text{chem}}.$$

We adopt log-uniform priors

$$C_{\text{geo}} \in [1, 10^4], \quad C_{\text{morph}} \in [1, 10^3], \quad C_{\text{chem}} \in [1, 10^3],$$

and stress-test up to  $10^6$ ,  $10^4$ , and  $10^4$ , respectively, to explore the limits of natural explanations.

## 2.4 Monte Carlo Sensitivity and Selection Effects

We perform Monte Carlo simulations with  $5 \times 10^4$  samples per scenario. For each realization, we draw  $P_i$  as described above, generate correlation multipliers  $C_{\text{geo}}$ ,  $C_{\text{morph}}$ ,  $C_{\text{chem}}$ , and compute an effective grouped probability

$$P_{\rm grp} = C_{\rm geo} \, P_{\rm geo} \times C_{\rm morph} \, P_{\rm morph} \times C_{\rm chem} \, P_{\rm chem},$$

where each grouped term is the product of the relevant  $P_i$ 's within that domain. In the updated anomaly set, the geometry/targeting domain contains  $E_1$ ,  $E_2$ ,  $E_3$ ,  $E_6$ , and  $E_7$ ; the morphology/photometry/polarization domain contains  $E_4$ ,  $E_8$ ,  $E_{10}$ ,  $E_{11}$ , and  $E_{12}$ ; and the chemistry/composition/dynamics domain contains  $E_5$ ,  $E_9$ , and  $E_{13}$ .

Survey selection is modeled by an effective number of discovery opportunities  $N_{\text{eff}}$ , sampled among  $\{500, 2000, 10^6, 10^8\}$  to bracket realistic and stress-test regimes, motivated by

comet discovery statistics and forward modeling for Rubin/LSST (Eldadi and Loeb, 2025; Trivedi and Loeb, 2025). The selection-adjusted probability is

$$P_{\text{sel}} = \min(1, N_{\text{eff}} P_{\text{grp}}).$$

Thus,  $P_{\text{sel}}$  represents the overall chance that surveys would have encountered an object with anomalies at least as extreme as those of 3I/ATLAS under the natural hypothesis.

### 3 Results

### 3.1 Take 1: Independent Loeb Anomalies

Under strict independence with the nominal means given above, the joint probability of the thirteen anomalies is

$$P_{\text{joint}} = \prod_{i=1}^{13} P_i \simeq 2.4 \times 10^{-30},$$

to within the uncertainty associated with interpreting the quoted bounds as priors. The required inflation factor to reconcile this with near-certainty is

$$k_{\rm req} = \frac{1}{P_{\rm joint}} \simeq 4.2 \times 10^{29},$$

or equivalently, nature would need  $\sim 4 \times 10^{29}$  independent attempts to produce one object as extreme as 3I/ATLAS by chance alone. Relative to earlier twelve-anomaly analyses, Loeb's updated anomaly list and probabilities strengthen the improbability by roughly a factor of 25.

# 3.2 Take 2: Grouped Correlations

When allowing for generous domain-level correlations, e.g.

$$C_{\rm geo} = 10^6, \quad C_{\rm morph} = 10^3, \quad C_{\rm chem} = 10^3,$$

the grouped probability  $P_{\rm grp}$  increases substantially compared to the pure-independence case but remains many orders of magnitude below unity. Depending on the particular draw of the  $P_i$ 's and correlation factors,  $P_{\rm grp}$  typically lies in the range  $\sim 10^{-12}$ – $10^{-8}$ . Even under these extreme correlation assumptions, the probability that all thirteen anomalies co-occur in a single object without invoking survey selection remains extremely low.

#### 3.3 Take 3: Selection Effects

Adopting  $N_{\rm eff}$  from comet discovery statistics and projected survey yields, we find that survey selection alone cannot compensate for the extremely small joint probability of the anomalies. For all values in our grid,  $N_{\rm eff} \in \{500, 2000, 10^6, 10^8\}$ , the resulting  $P_{\rm sel}$  values remain many orders of magnitude below the 1% plausibility threshold in both the baseline and stress configurations. In other words, even if we grant the most optimistic discovery opportunities consistent with current and near-future surveys, chance encounters with an object as extreme as 3I/ATLAS remain extraordinarily unlikely.

### 3.4 Take 4: Cross-Domain Coupling

Achieving  $P_{\rm sel} > 1\%$  requires a combined inflation factor

$$K_{\rm nat} = C_{\rm geo} C_{\rm morph} C_{\rm chem} N_{\rm eff} \gtrsim 2 \times 10^{17},$$

which lies well outside the range supported by current comet statistics and survey modeling. Only when both the correlation multipliers and  $N_{\rm eff}$  are pushed into exaggerated regimes—e.g.  $C_{\rm geo} \sim 10^6$ ,  $C_{\rm morph} \sim 10^4$ ,  $C_{\rm chem} \sim 10^4$ , and  $N_{\rm eff} \sim 10^8$ —do a non-negligible fraction of Monte Carlo realizations approach the 1% plausibility threshold; in our updated runs, even these stress scenarios fail to produce any exceedances.

### 3.5 Monte Carlo Sensitivity

Baseline simulations show no exceedance of the 1% plausibility threshold for any value of  $N_{\rm eff} \leq 10^8$ . In fact, across  $5 \times 10^4$  Monte Carlo realizations for each  $N_{\rm eff}$ , not a single draw produced  $P_{\rm sel} \geq 1\%$ , even in the stress runs with extreme correlation factors and  $N_{\rm eff} = 10^8$  (Table 1). This implies an empirical upper bound of order  $2 \times 10^{-5}$  on the exceedance probability in both the baseline and stress ensembles. The probability mass in Figure 1 therefore lies entirely in a regime that is comfortably below the 1% plausibility line.

For non-specialist readers, a more quantitative dice analogy is helpful. Consider a fair 20-sided die rolled only 20 times. The chance that the *same face* appears on all 20 rolls is

$$P_{20\text{die}} = \frac{1}{20^{19}} \approx \frac{1}{5 \times 10^{21}}.$$

In other words, you would expect to see such a perfect run (all rolls showing the same face) only once in about five billion trillion experiments of 20 throws each. The updated combined anomalies of 3I/ATLAS are at least this unlikely under the natural models we test, unless one assumes an enormous number of unseen trials or some mechanism that biases the outcomes.

$N_{ m eff}$	Baseline exceedance $(P_{\rm sel} \ge 1\%)$	Stress exceedance $(P_{\rm sel} \ge 1\%)$
500	0.0%	0.0%
2000	0.0%	0.0%
$10^{6}$	0.0%	0.0%
$10^{8}$	0.0%	0.0%

Table 1: Exceedance rates for the selection-adjusted probability  $P_{\rm sel}$  under baseline and stress assumptions, using the thirteen updated Loeb anomalies as the event set. None of the  $5 \times 10^4$  Monte Carlo realizations for any  $N_{\rm eff}$  reached the 1% plausibility threshold, implying an empirical upper bound of  $\lesssim 2 \times 10^{-5}$  on the exceedance probability in both baseline and stress scenarios.

To quantify not only exceedance frequencies but also the typical scale of  $P_{\rm sel}$  values, we computed the median, 90th percentile, and 99th percentile of  $P_{\rm sel}$  for each  $N_{\rm eff}$  in both the baseline and stress ensembles (each with  $5\times 10^4$  realizations). In the baseline runs, the median  $P_{\rm sel}$  ranges from  $\sim 2\times 10^{-23}$  for  $N_{\rm eff}=5\times 10^2$  to  $\sim 4\times 10^{-18}$  for  $N_{\rm eff}=10^8$ , with

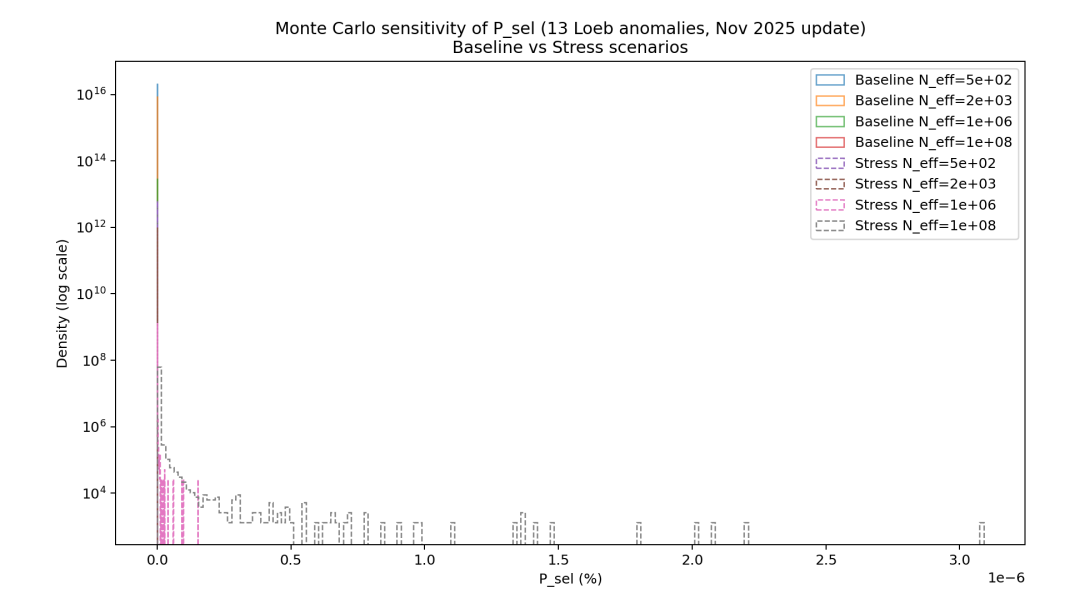


Figure 1: Monte Carlo density of  $P_{\rm sel}$  (expressed in percent) for the thirteen updated Loeb anomalies (November 2025 list).  $P_{\rm sel}$  is the selection-adjusted probability of observing all thirteen anomalies of 3I/ATLAS, combining independent improbabilities with correlation factors and the effective number of survey opportunities  $N_{\rm eff}$ . Solid lines show baseline assumptions, dashed lines show stress scenarios with extreme correlations. The distribution mass remains well below the 1% plausibility threshold in realistic regimes.

99th percentiles remaining below  $\sim 7 \times 10^{-14}$  for all  $N_{\rm eff}$ . In the stress runs, the medians increase modestly, from  $\sim 2 \times 10^{-21}$  at  $N_{\rm eff} = 5 \times 10^2$  to  $\sim 4 \times 10^{-16}$  at  $N_{\rm eff} = 10^8$ , and the most extreme 99th-percentile value occurs for  $N_{\rm eff} = 10^8$  with  $P_{\rm sel} \approx 1.8 \times 10^{-10}$  (i.e.  $\approx 1.8 \times 10^{-8}\%$ ). Thus, even the upper tail of the stress ensemble remains many orders of magnitude below the 1% plausibility threshold, consistent with the zero-exceedance rates reported in Table 1.

# 4 Discussion

Our updated results highlight the extraordinary improbability of the simultaneous occurrence of the thirteen Loeb anomalies reported for 3I/ATLAS. Each anomaly considered separately—CO<sub>2</sub> dominance with suppressed water (Cordiner et al., 2025; Xing et al., 2025), Ni-rich composition with extreme Ni/CN ratios (Rahatgaonkar et al., 2025; Puzia et al., 2025; Hoogendam et al., 2025), excess CN behavior and early onset (Manzano-King et al., 2025), steep and unusual brightening behavior near perihelion (Tonry et al., 2025; Zhang, 2025), sunward and anti-solar jets with weak dust tails (Jewitt et al., 2025; Santana-Ros et al., 2025; Keto and Loeb, 2025), extreme negative polarization (Gray et al., 2025), the tension between non-gravitational acceleration and an intact nucleus (Cloete et al., 2025; Jewitt et al., 2025), and now the fine-tuned Jupiter Hill-radius encounter and multi-planet geometry—has potential natural explanations. However, these explanations are largely domain-specific and

uncorrelated.

Alternative explanations invoking survey biases, geometric coincidences in arrival direction and timing, or unusually strong physical correlations between otherwise independent domains can improve plausibility but fall short by many orders of magnitude in our Monte Carlo ensemble. Stress scenarios show that even with  $N_{\rm eff}=10^8$  and maximally generous cross-domain correlations, the simulated values of  $P_{\rm sel}$  remain below the 1% level in all  $5\times10^4$  realizations. In other words, the stress configuration does not produce a single case in which an object with anomalies at least as extreme as 3I/ATLAS would be considered even mildly plausible under the natural hypothesis. Such assumptions would require humanity to have effectively sampled tens or hundreds of millions of ISO-like objects already, contradicting the current observational record.

The Loeb Scale provides a useful interpretive lens for these results (Eldadi and Loeb, 2025; Trivedi and Loeb, 2025). By construction, Level 4 marks the point where a technological origin must be seriously considered alongside natural hypotheses. 3I/ATLAS comfortably reaches this level (and arguably higher) on the basis of its anomaly set alone. Our Bayesian analysis complements the Loeb Scale by quantifying how strongly the combined anomalies disfavour simple natural models under reasonable priors.

Beyond the physical anomalies, data policy and communication have also influenced the discussion. Delays or ambiguities in releasing spectroscopic and imaging data from space-based assets have fueled speculation that the full picture may be even more puzzling than the already published results suggest. While such sociological factors lie outside the scope of our Bayesian model, they add to the perception that 3I/ATLAS is not a typical comet.

Intentional origin, while extraordinary, remains a parsimonious explanation in the sense that it offers a single common-cause mechanism that can, in principle, account for geometry, timing, morphology, composition, polarization, and dynamics simultaneously. A natural explanation would need to provide a comparably unified account, together with a credible population model in which such objects are expected to appear with non-negligible probability. The real unavoidable key question is: What realistic generative process—natural or not—actually makes it easy to get this whole bundle of features at once?

# 5 Conclusions

The conjunction of the thirteen updated Loeb anomalies in 3I/ATLAS has a joint probability  $P_{\rm joint} \simeq 2.4 \times 10^{-30}$  under the assumption of independence, using Loeb's November 2025 probability estimates as nominal means. Even after allowing for generous domain-level correlations and optimistic survey selection  $(N_{\rm eff})$ , natural models require inflation factors  $K_{\rm nat} \gtrsim 10^{17}$  to approach  $P_{\rm sel} \gtrsim 1\%$ . Monte Carlo sensitivity tests confirm that this conclusion is robust to reasonable perturbations of the priors, with zero exceedances of the 1% plausibility threshold in  $5 \times 10^4$  realizations for each  $N_{\rm eff}$  in both baseline and stress ensembles.

In terms of the Loeb Scale, our analysis supports the view that 3I/ATLAS occupies a regime in which intentional origin must be weighed seriously against natural hypotheses. Future work could refine the anomaly definitions, tighten probability estimates as more data become available, and incorporate more detailed physical models. Absent such developments,

however, the Bayesian evidence strongly disfavors a purely natural explanation that treats the anomalies as coincidental. Put differently, the real unavoidable key question for any proposed model is: What realistic generative process—natural or artificial—makes it straightforward rather than miraculous to produce the full thirteen-anomaly bundle observed in 3I/ATLAS?

### References

- Bolin, B. T. et al. (2025). Physical properties of interstellar comet 3i/atlas. *Monthly Notices of the Royal Astronomical Society*. in press.
- Cloete, K. et al. (2025). Upper limits on the nucleus mass and non-gravitational acceleration of 3i/atlas. Astronomy & Astrophysics.
- Cordiner, M. A., Roth, N. X., Kelley, M. S. P., et al. (2025). Jwst detection of a carbon dioxide dominated gas coma surrounding interstellar object 3i/atlas. Astronomy & Astrophysics.
- De la Fuente Marcos, R. and De la Fuente Marcos, C. (2025). On the dynamical origin of interstellar comet 3i/atlas. Astronomy & Astrophysics.
- Eldadi, O. and Loeb, A. (2025). The loeb scale: Astronomical classification of interstellar objects. arXiv e-prints.
- Gray, M. et al. (2025). Extreme negative polarization of interstellar comet 3i/atlas. *Monthly Notices of the Royal Astronomical Society*.
- Hibberd, A., Siraj, A., and Loeb, A. (2025). Is the interstellar object 3i/atlas alien technology? *Astrophysical Journal*. submitted.
- Hoogendam, A., Loeb, A., et al. (2025). Nickel and cyanogen in the gas plume of interstellar comet 3i/atlas. Astrophysical Journal Letters.
- Jewitt, D., Hui, M.-T., Mutchler, M., Kim, Y., and Agarwal, J. (2025). Hubble space telescope observations of the interstellar interloper 3i/atlas. *Astrophysical Journal Letters*.
- Keto, E. and Loeb, A. (2025). The physics of cometary anti-tails and application to 3i/atlas. *Astrophysical Journal*.
- Loeb. Α. (2025a).The 12th anomaly 3i/atlas: Orientation ofof the smeared by rotation. https://medium.com/@avi-loeb/ the-12th-anomaly-of-3i-atlas-orientation-of-the-jets-is-not-smeared-by-rotation-30035 Medium article.
- Loeb, A. (2025b). 3i/atlas and the wow! signal. https://avi-loeb.medium.com/the-wow-signal-and-3i-atlas-xxxx. Medium article discussing sky-direction coincidence.

- Loeb, A. (2025c). Afterthoughts on the non-gravitational acceleration of 3i/atlas. https://avi-loeb.medium.com/afterthoughts-on-the-non-gravitational-acceleration-of-3i-atlas-41cf3f54aaf9. Medium article.
- Loeb, A. (2025d). Anomalies of 3i/atlas, organized by likelihood. https://avi-loeb.medium.com/anomalies-of-3i-atlas-organized-by-likelihood-af20fb3b6d21. Medium article, accessed 23 November 2025.
- Manzano-King, C. et al. (2025). Early cn onset and carbon-chain depletion in interstellar object 3i/atlas. Astronomy & Astrophysics. submitted.
- Puzia, T. H. et al. (2025). Optical spectroscopy of 3i/atlas: Nickel emission in the absence of iron. *Astrophysical Journal*. submitted.
- Rahatgaonkar, S. et al. (2025). Vlt spectroscopy of interstellar comet 3i/atlas: Metal lines and composition. Astronomy & Astrophysics. submitted.
- Santana-Ros, T. et al. (2025). Temporal evolution and jet morphology of interstellar comet 3i/atlas. Astronomy & Astrophysics. submitted.
- Seligman, D. Z., Micheli, M., Farnocchia, D., et al. (2025). Discovery and preliminary characterization of a third interstellar object: 3i/atlas. *Astrophysical Journal Letters*, 989:L36.
- Taylor, A. G. et al. (2025). Kinematic age and possible birth environment of interstellar object 3i/atlas. *Astrophysical Journal*. submitted.
- Tonry, J. et al. (2025). Atlas photometry of 3i/atlas: Rapid brightening and color evolution. Astrophysical Journal. submitted.
- Trivedi, O. and Loeb, A. (2025). Quantitative mapping of the loeb scale. arXiv e-prints.
- Xing, Z., Oset, S., Noonan, J., and Bodewits, D. (2025). Water detection in the interstellar object 3i/atlas. Astrophysical Journal Letters.
- Zhang, Y. (2025). Rapid brightening and photometric behavior of interstellar comet 3i/atlas near perihelion. Astrophysical Journal Letters.